AA-stacked bilayer graphene in an applied electric field: Tunable antiferromagnetism and coexisting exciton order parameter

R. S. Akzyanov,[1,2,3] A. O. Sboychakov,[2,4] A. V. Rozhkov,[1,2,4] A. L. Rakhmanov,[1,2,3,4] and Franco Nori[4,5]

[1]*Moscow Institute of Physics and Technology, Dolgoprudny, Moscow Region, 141700 Russia*

[2]*Institute for Theoretical and Applied Electrodynamics, Russian Academy of Sciences, Moscow, 125412 Russia*

[3]*All-Russia Research Institute of Automatics, Moscow, 127055 Russia*

[4]*CEMS, RIKEN, Saitama, 351-0198 Japan*

[5]*Department of Physics, University of Michigan, Ann Arbor, Michigan 48109-1040, USA*

We study the electronic properties of *AA*-stacked bilayer graphene in a transverse electric field. The strong on-site Coulomb repulsion stabilizes the antiferromagnetic order in such a system. The antiferromagnetic order is suppressed by the transverse bias voltage, at least partially. The interplane Coulomb repulsion and nonzero voltage stabilize an exciton order parameter. The exciton order parameter coexists with the antiferromagnetism and can be as large as several tens of meV for realistic values of the bias voltage and interaction constants. The application of a transverse bias voltage can be used to control the transport properties of the bilayer.

PACS number(s): 73.22.Pr, 73.22.Gk, 73.21.Ac

I. INTRODUCTION

The electronic properties of graphene are a subject of active theoretical and experimental studies [1–3]. In addition to single-layer graphene, bilayer graphene also attracts significant research attention. This interest is partly driven by the desire to extend the family of graphenelike materials and to create materials with a controllable gap in the electronic spectrum.

The most studied form of bilayer is the *AB* (or Bernal) stacked bilayer graphene (*AB*-BLG) [4–8]. The biased *AB*-BLG has a tunable gap [9,10]. Excitons can exist in the *AB*-BLG under certain conditions [11,12].

The *AA*-stacked bilayer graphene (*AA*-BLG) has received less attention [13–22]. However, samples of *AA*-BLG have recently been produced [17–19] and a detailed study of this system becomes necessary. A significant feature of the *AA*-BLG is the perfect nesting of the hole and electron Fermi surfaces. These degenerate Fermi surfaces are unstable with respect of an arbitrarily weak electron interaction, and the *AA*-BLG becomes an antiferromagnetic (AFM) insulator with a finite electron gap [20]. This electronic instability is strongest at zero doping, when the bands cross at the Fermi level.

An interesting phenomenon, which occurs in bilayer graphene systems, is exciton condensation [23,24]. In graphene bilayers, exciton condensation attracted attention for both fundamental reasons [25–29] and possible applications in devices, including ultrafast switches and dispersionless field-effect transistors [30].

The purpose of this paper is to investigate the influence of a transverse electric field on the properties of the *AA*-BLG. We show that such a field can partially suppress the AFM order parameter. However, the degree of suppression heavily depends on the effective value of the on-site Coulomb repulsion. Moreover, the transverse bias stabilizes the exciton order parameter. Namely, we found that the exciton order parameter coexists with the AFM order if a transverse electric field is applied. The exciton order is tuned by the voltage and tied to the AFM order. Since the magnitude of the gap is sensitive to the transverse field, it appears possible to control

the transport properties of the bilayer with the help of a transverse bias, which can be created by, e.g., a gate electrode.

The paper is organized as follows. In Sec. II we analyze the single-electron part of our model. Within the tight-binding approach we derive the degenerate electronic spectrum of the model. In Sec. III we consider the on-site and intersite interplane Coulomb repulsion using a mean-field theory. The electronic interaction removes the degeneracy of the single-electron spectrum creating a gap. We found that the phase with coexisting AFM and exciton orders is the most stable one. We obtain the equations for the order parameters and solve them using both analytic and numerical methods. The effect of doping is discussed.

II. TIGHT-BINDING HAMILTONIAN

The crystal structure of the *AA*-BLG is shown in Fig. 1. The *AA*-BLG consists of two graphene layers, up and down. Each carbon atom of the upper layer is located above the corresponding atom of the lower layer. Each layer consists of two triangular sublattices $\mathcal{A}$ and $\mathcal{B}$. The elementary unit cell of the *AA*-BLG contains four carbon atoms $A1$, $A2$, $B1$, and $B2$.

We write the single-particle tight-binding Hamiltonian of the *AA*-BLG in the form

$$
\begin{aligned}
H_0 = &-t \sum_{\langle \mathbf{nm}\rangle i\sigma} (d^\dagger_{\mathbf{n}i\mathcal{A}\sigma} d_{\mathbf{m}i\mathcal{B}\sigma} + \text{H.c.}) \\
&+ t_0 \sum_{\mathbf{n}a\sigma} (d^\dagger_{\mathbf{n}1a\sigma} d_{\mathbf{n}2a\sigma} + \text{H.c.}) \\
&+ \frac{V_0}{2} \sum_{\mathbf{n}a\sigma} (d^\dagger_{\mathbf{n}1a\sigma} d_{\mathbf{n}1a\sigma} - d^\dagger_{\mathbf{n}2a\sigma} d_{\mathbf{n}2a\sigma}).
\end{aligned}
\tag{1}
$$

Here $d^\dagger_{\mathbf{n}ia\sigma}$ and $d_{\mathbf{n}ia\sigma}$ are the creation and annihilation operators of an electron with spin projection σ in the layer $i = 1,2$ on the sublattice $a = \mathcal{A},\mathcal{B}$ at the position $\mathbf{n}$, and $\langle ...\rangle$ denotes a nearest-neighbor pair inside a layer. The amplitude t (t_0) in Eq. (1) describes the in-plane (interplane) nearest-neighbor hopping, and V_0 is the voltage applied perpendicular to the
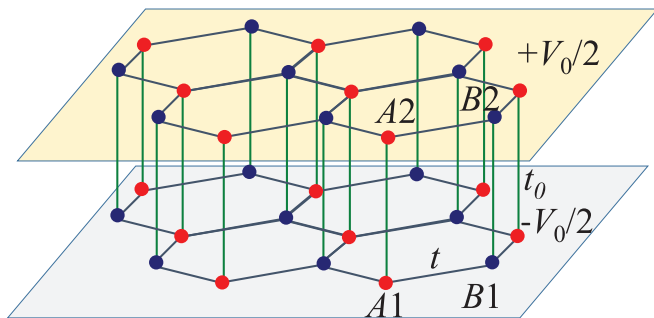
FIG. 1. (Color online) Crystal structure of the AA-stacked bilayer graphene. The circles denote carbon atoms in the $\mathcal{A}$ (red) and $\mathcal{B}$ (blue) sublattices in the bottom (1), in gray, and top (2), in yellow, layers. The unit cell of the AA-BLG consists of four atoms $A1$, $A2$, $B1$, and $B2$. The hopping integrals t and t_0 correspond to the in-plane and interplane nearest-neighbor hopping. A transverse electrical voltage V_0 is applied to the planes.

layers. We assume that $V_0 \ll t$, which corresponds to typical experimental conditions [9,10]. For calculations, we use the values of the hopping integrals $t = 2.57$ eV, $t_0 = 0.36$ eV, computed by the dynamical field theory (DFT) method for multilayer carbon systems in Ref. [31].

After diagonalizing the Hamiltonian (1) we obtain four bands $\varepsilon_{0\mathbf{k}}^{(s)}$ ($s = 1, \ldots, 4$), which can be written as

$$\varepsilon_{0\mathbf{k}}^{(1)} = -\sqrt{t_0^2 + \frac{V_0^2}{4}} - t\zeta_{\mathbf{k}}, \quad \varepsilon_{0\mathbf{k}}^{(2)} = -\sqrt{t_0^2 + \frac{V_0^2}{4}} + t\zeta_{\mathbf{k}},$$

$$\varepsilon_{0\mathbf{k}}^{(3)} = \sqrt{t_0^2 + \frac{V_0^2}{4}} - t\zeta_{\mathbf{k}}, \quad \varepsilon_{0\mathbf{k}}^{(4)} = \sqrt{t_0^2 + \frac{V_0^2}{4}} + t\zeta_{\mathbf{k}}, \quad (2)$$

where

$$\zeta_{\mathbf{k}} = |f_{\mathbf{k}}|, \quad f_{\mathbf{k}} = 1 + 2\exp\left(\frac{3ik_x a_0}{2}\right)\cos\left(\frac{\sqrt{3}k_y a_0}{2}\right), \quad (3)$$

and $a_0 = 1.42$ Å is the in-plane carbon-carbon distance. The bands $s = 2$ and 3 cross the Fermi level near the Dirac points $\mathbf{K} = 2\pi(\sqrt{3}, 1)/(3\sqrt{3}a_0)$ and $\mathbf{K}' = 2\pi(\sqrt{3}, -1)/(3\sqrt{3}a_0)$. As it follows from Eqs. (2), the band $s = 2$ is electronlike, while the band $s = 3$ is holelike. The band $s = 1$ lies below and the band $s = 4$ lies above the Fermi energy and, consequently, they do not form a Fermi surface.

In contrast to the Bernal stacking (where the bias voltage opens a gap at the Fermi level [9,10]), the application of a transverse bias voltage does not qualitatively change the spectrum of the AA-BLG. The Fermi surface is given by the equation $\zeta_{\mathbf{k}} = t^{-1}\sqrt{t_0^2 + V_0^2/4} = \zeta_0$. Since $\zeta_0 \ll 1$, we can expand the function $\zeta_{\mathbf{k}}$ near the Dirac points and find that the Fermi surface consists of two circles with radius $k_r = 2\zeta_0/(3a_0)$.

One of the most important features of this tight-binding band structure is that the Fermi surfaces of both bands coincide. That is, the electron and hole components of the Fermi surface are perfectly nested. This property of the Fermi surface is quite robust against changes in the tight-binding Hamiltonian. It survives even if longer-range hoppings are taken into account,

or a system with two nonequivalent layers is considered (e.g., the single-side hydrogenated graphene [32]). However, the electron interactions can remove the degeneracy in the spectrum, creating a finite gap [20].

III. ELECTRON-ELECTRON INTERACTION

The electronic spectrum changes drastically when considering the Coulomb interaction. To study the effects of this interaction on the electronic properties of our system, we use the following Hubbard-like Hamiltonian:

$$H_{\text{int}} = H_{\text{U}} + H_{\text{V}}. \quad (4)$$

The first term, H_{U}, is the on-site Coulomb repulsion between the electrons:

$$H_{\text{U}} = U_0 \sum_{\mathbf{n}ia}\left(n_{\mathbf{n}ia\uparrow} - \frac{1}{2}\right)\left(n_{\mathbf{n}ia\downarrow} - \frac{1}{2}\right), \quad (5)$$

where $n_{\mathbf{n}ia\sigma} = d_{\mathbf{n}ia\sigma}^{\dagger}d_{\mathbf{n}ia\sigma}$ is the operator of the occupation number. The second term, H_{V}, describes the nearest-neighbor Coulomb repulsion. It has the form

$$H_{\text{V}} = U_{12}\sum_{\substack{\mathbf{n}a \\ \sigma\sigma'}}\left(n_{\mathbf{n}1a\sigma} - \frac{1}{2}\right)\left(n_{\mathbf{n}2a\sigma'} - \frac{1}{2}\right)$$

$$+ U_{ab}\sum_{\substack{\langle \mathbf{nm}\rangle \\ i\sigma\sigma'}}\left(n_{\mathbf{n}i\mathcal{A}\sigma} - \frac{1}{2}\right)\left(n_{\mathbf{m}i\mathcal{B}\sigma'} - \frac{1}{2}\right), \quad (6)$$

where the first term is the nearest-neighbor interaction between the electrons in different layers, while the second term describes the in-plane nearest-neighbor interaction. The terms $1/2$ in the brackets in Eqs. (5) and (6) are added to keep the chemical potential corresponding to the half filling (zero doping) equal to zero.

The value of the electron-electron interaction in graphene is relatively strong. According to DFT calculations [33], the on-site repulsion energy, U_0, is about 9–10 eV, while the in-plane intersite repulsion, U_{ab}, is about 5–6 eV. The nearest-neighbor interplane interaction in the bilayer graphene is unknown. We can estimate it as $U_{12} \approx U_{ab}a_0/c \approx 2.5$ eV, where $c = 3.35$ Å is the distance between the layers. It is commonly accepted that the mean-field calculations overestimate the resulting value of the antiferromagnetic (AFM) order parameter driven by the electron-electron interaction. In addition, the long-range Coulomb interaction can effectively reduce [34] the on-site repulsion energy U_0. Keeping all this in mind, we use for further estimates the values of U_0, U_{ab}, and U_{12} smaller than those obtained in the DFT calculations. We will use $U_0/t \simeq 2$–3.5, $U_{ab}/t \simeq 1$–2, and $U_{12}/t \simeq 0.5$–1.

A. Mean-field equations

We analyze the properties of the total Hamiltonian $H = H_0 + H_{\text{int}}$ in the mean-field approximation. It was shown previously for zero-bias voltage that the on-site Coulomb repulsion stabilizes the AFM ground state in the AA-BLG [20–22]. We will show below that the AFM order also exists for $V_0 \neq 0$. We fix the spin quantization z axis perpendicular to the layers in the xy plane. In this case the AFM order parameter

can be written as

$$\Delta_{\mathrm{AFM}}^{ia} = \frac{U_0}{2}(\langle d_{\mathbf{n}ia\uparrow}^\dagger d_{\mathbf{n}ia\uparrow}\rangle - \langle d_{\mathbf{n}ia\downarrow}^\dagger d_{\mathbf{n}ia\downarrow}\rangle), \tag{7}$$

$$\Delta_{\mathrm{AFM}}^{1\mathcal{A}} = \Delta_{\mathrm{AFM}}^{2\mathcal{B}} = -\Delta_{\mathrm{AFM}}^{1\mathcal{B}} = -\Delta_{\mathrm{AFM}}^{2\mathcal{A}} \equiv \Delta_{\mathrm{AFM}}, \tag{8}$$

and the Δ_{AFM} is real. Such an AFM order, when the spin at any given site is antiparallel to spins at all its nearest-neighbor sites, is referred to as *G*-type AFM. In the mean-field approximation, the on-site interaction Hamiltonian, H_{U}, takes the form

$$H_{\mathrm{U}}^{\mathrm{MF}} = -\frac{\mathcal{N}U_0\Delta n^2}{4} + \frac{U_0\Delta n}{4}\sum_{\mathbf{n}a\sigma}(n_{\mathbf{n}1a\sigma} - n_{\mathbf{n}2a\sigma})$$
$$+ \frac{4\mathcal{N}\Delta_{\mathrm{AFM}}^2}{U_0} - \sum_{\mathbf{n}ia}\Delta_{\mathrm{AFM}}^{ia}(n_{\mathbf{n}ia\uparrow} - n_{\mathbf{n}ia\downarrow}), \tag{9}$$

where $\Delta n = \sum_\sigma(\langle n_{\mathbf{n}1a\sigma}\rangle - \langle n_{\mathbf{n}2a\sigma}\rangle)$ is the difference in the electron densities in two graphene layers induced by the applied voltage V_0 and $\mathcal{N}$ is the number of unit cells in the sample.

Let us consider now the intersite part of the interaction. The Hamiltonian H_{int} can produce several order parameters in the system. However, for zero-bias voltage all of them compete with the antiferromagnetism and only the antiferromagnetic order parameter survives, because U_0 is the strongest interaction constant. A non-zero-bias voltage breaks the symmetry between two graphene layers. In this case, there exists an order parameter driven by the interlayer interaction, which coexists with antiferromagnetism. An analysis based on symmetry considerations, similar to that presented in Ref. [20], shows that this order parameter should have the form

$$\Delta_{\mathrm{exc}}^a = \frac{U_{12}}{2}(\langle d_{\mathbf{n}1a\uparrow}^\dagger d_{\mathbf{n}2a\uparrow}\rangle - \langle d_{\mathbf{n}1a\downarrow}^\dagger d_{\mathbf{n}2a\downarrow}\rangle), \tag{10}$$

$$\Delta_{\mathrm{exc}}^{\mathcal{A}} = -\Delta_{\mathrm{exc}}^{\mathcal{B}} \equiv \Delta_{\mathrm{exc}}, \tag{11}$$

and the Δ_{exc} is real. This order parameter corresponds to the bound state of the electron and the hole in different layers. We call it the exciton order parameter. The mean-field expression for the intersite part of the Hamiltonian has the following form:

$$H_{\mathrm{V}}^{\mathrm{MF}} = \mathcal{N}\left[-\frac{(3U_{ab}-U_{12})\Delta n^2}{2} + \frac{4\Delta_{\mathrm{exc}}^2}{U_{12}}\right]$$
$$+ \frac{(3U_{ab}-U_{12})\Delta n}{2}\sum_{\mathbf{n}a\sigma}(n_{\mathbf{n}1a\sigma} - n_{\mathbf{n}2a\sigma})$$
$$- \sum_{\mathbf{n}a\sigma}\left[\Delta_{\mathrm{exc}}^a(d_{\mathbf{n}1a\uparrow}^\dagger d_{\mathbf{n}2a\uparrow} - d_{\mathbf{n}1a\downarrow}^\dagger d_{\mathbf{n}2a\downarrow}) + \mathrm{H.c.}\right]. \tag{12}$$

We introduce the four-component spinor

$$\psi_{\mathbf{k}\sigma}^\dagger = (d_{\mathbf{k}1\mathcal{A}\sigma}^\dagger, d_{\mathbf{k}2\mathcal{A}\sigma}^\dagger, d_{\mathbf{k}1\mathcal{B}\sigma}^\dagger, d_{\mathbf{k}2\mathcal{B}\sigma}^\dagger). \tag{13}$$

In terms of this spinor, the mean field Hamiltonian

$$H^{\mathrm{MF}} = H_0 + H_{\mathrm{U}}^{\mathrm{MF}} + H_{\mathrm{V}}^{\mathrm{MF}} \tag{14}$$

can be written as

$$H^{\mathrm{MF}} = \mathcal{N}E_0 + \sum_{\mathbf{k}\sigma}\psi_{\mathbf{k}\sigma}^\dagger(\hat{H}_{0\mathbf{k}} + \hat{\Delta}_\sigma)\psi_{\mathbf{k}\sigma}, \tag{15}$$

where E_0 is a *c* number,

$$E_0 = -\frac{(U_0 + 6U_{ab} - 2U_{12})\Delta n^2}{4} + \frac{4\Delta_{\mathrm{AFM}}^2}{U_0} + \frac{4\Delta_{\mathrm{exc}}^2}{U_{12}}, \tag{16}$$

and $\hat{H}_{0\mathbf{k}}$ and $\hat{\Delta}_\sigma$ are the 4×4 matrices:

$$\hat{H}_{0\mathbf{k}} = -\begin{pmatrix} -V/2 & t_0 & tf_{\mathbf{k}} & 0 \\ t_0 & V/2 & 0 & tf_{\mathbf{k}} \\ tf_{\mathbf{k}}^* & 0 & -V/2 & t_0 \\ 0 & tf_{\mathbf{k}}^* & t_0 & V/2 \end{pmatrix}, \tag{17}$$

$$\hat{\Delta}_\uparrow = \begin{pmatrix} \Delta_{\mathrm{AFM}} & \Delta_{\mathrm{exc}} & 0 & 0 \\ \Delta_{\mathrm{exc}} & -\Delta_{\mathrm{AFM}} & 0 & 0 \\ 0 & 0 & -\Delta_{\mathrm{AFM}} & -\Delta_{\mathrm{exc}} \\ 0 & 0 & -\Delta_{\mathrm{exc}} & \Delta_{\mathrm{AFM}} \end{pmatrix},$$

$$\hat{\Delta}_\downarrow = -\hat{\Delta}_\uparrow. \tag{18}$$

In Eq. (17) the quantity V is the effective bias voltage given by the relation

$$V = V_0 + \alpha\Delta n, \quad \alpha = \frac{U_0 + 6U_{ab} - 2U_{12}}{2} > 0. \tag{19}$$

This equation describes the screening of the applied voltage due to the electron-electron interaction. Indeed, since $\Delta n < 0$ for $V_0 > 0$, we have $V < V_0$. For the parameters U_0, U_{ab}, and U_{12} under study the constant α can be estimated as $3.5t$–$7t$.

The mean-field spectrum is obtained by the diagonalization of two 4×4 matrices in Eq. (15). It consists of four bands doubly degenerate with respect to spin:

$$\varepsilon_{\mathbf{k}}^{(1)} = -\sqrt{A_{\mathbf{k}} + 2B_{\mathbf{k}}}, \quad \varepsilon_{\mathbf{k}}^{(2)} = -\sqrt{A_{\mathbf{k}} - 2B_{\mathbf{k}}},$$
$$\varepsilon_{\mathbf{k}}^{(3)} = \sqrt{A_{\mathbf{k}} - 2B_{\mathbf{k}}}, \quad \varepsilon_{\mathbf{k}}^{(4)} = \sqrt{A_{\mathbf{k}} + 2B_{\mathbf{k}}}, \tag{20}$$

where

$$A_{\mathbf{k}} = \Delta_{\mathrm{AFM}}^2 + \Delta_{\mathrm{exc}}^2 + t^2\zeta_{\mathbf{k}}^2 + t_0^2 + \frac{V^2}{4},$$
$$B_{\mathbf{k}} = \sqrt{\left[-\Delta_{\mathrm{exc}}t_0 + \Delta_{\mathrm{AFM}}\frac{V}{2}\right]^2 + t^2\zeta_{\mathbf{k}}^2\left[t_0^2 + \frac{V^2}{4}\right]}. \tag{21}$$

The full gap in the spectrum Δ is defined as $\Delta = \min_{\mathbf{k}}(\varepsilon_{\mathbf{k}}^{(3)} - \varepsilon_{\mathbf{k}}^{(2)})/2$. It relates to the AFM and exciton order parameters as

$$\Delta = \frac{2\Delta_{\mathrm{AFM}}t_0 + \Delta_{\mathrm{exc}}V}{\sqrt{4t_0^2 + V^2}}. \tag{22}$$

To determine the values of the order parameters Δ_{AFM} and Δ_{exc} we should minimize the grand potential Ω. The grand potential per unit cell is

$$\Omega = E_0 - 2T\sum_{s=1}^4\int\frac{d\mathbf{k}}{V_{\mathrm{BZ}}}\ln\left[1 + e^{-\varepsilon_{\mathbf{k}}^{(s)}/T}\right], \tag{23}$$

where V_{BZ} is the volume of the first Brillouin zone.

To calculate the integrals over the Brillouin zone, it is convenient to introduce the density of states:

$$\rho_0(\zeta) = \int\frac{d\mathbf{k}}{V_{\mathrm{BZ}}}\delta(\zeta - \zeta_{\mathbf{k}}). \tag{24}$$

This function is nonzero only if $0 < \zeta < 3$. It is related to the single layer graphene density of states $\rho_{\mathrm{gr}}(\zeta)$ as $\rho_{\mathrm{gr}}(\zeta) = \rho_0(\zeta)/t$ (see Ref. [1]).

Minimization of Ω with respect to Δ_{AFM} and Δ_{exc} gives the equations

$$\frac{4\Delta_{\mathrm{AFM}}}{U_0} = \int_0^3 d\zeta\, \rho_0(\zeta) \left[\Delta_{\mathrm{AFM}} + \frac{V}{2}\theta(\zeta) \right] F(\varepsilon^{(1)}(\zeta))$$
$$+ \int_0^3 d\zeta\, \rho_0(\zeta) \left[\Delta_{\mathrm{AFM}} - \frac{V}{2}\theta(\zeta) \right] F(\varepsilon^{(2)}(\zeta)),$$
$$(25)$$

$$\frac{4\Delta_{\mathrm{exc}}}{U_{12}} = \int_0^3 d\zeta\, \rho_0(\zeta)[\Delta_{\mathrm{exc}} - t_0\theta(\zeta)] F(\varepsilon^{(1)}(\zeta))$$
$$+ \int_0^3 d\zeta\, \rho_0(\zeta)[\Delta_{\mathrm{exc}} + t_0\theta(\zeta)] F(\varepsilon^{(2)}(\zeta)), \quad (26)$$

where
$$F(\varepsilon) = \frac{f(-\varepsilon) - f(\varepsilon)}{\varepsilon}, \quad f(\varepsilon) = \frac{1}{e^{\varepsilon/T} + 1},$$
$$(27)$$
$$\theta(\zeta) = \frac{2\Delta_{\mathrm{exc}}t_0 - \Delta_{\mathrm{AFM}}V}{\sqrt{(2\Delta_{\mathrm{exc}}t_0 - \Delta_{\mathrm{AFM}}V)^2 + t^2(4t_0^2 + V^2)\zeta^2}},$$

and $\varepsilon^{(s)}(\zeta)$ are given by Eqs. (20) and (21), in which $\zeta_{\mathbf{k}}$ is replaced by ζ.

Equations (25) and (26) define the AFM and exciton order parameters as functions of the effective bias voltage V. In order to find the dependencies of Δ_{AFM} and Δ_{exc} on the applied voltage V_0 we should use Eq. (19). To find the charge imbalance between two graphene layers Δn, we apply the Hellman-Feynman theorem [35]:

$$\Delta n = 2\left\langle \frac{\partial H^{\mathrm{MF}}}{\partial V} \right\rangle = 2\frac{\partial E}{\partial V}, \quad (28)$$

where E is the energy of the system per unit cell. It can be written as

$$E = E_0 + \sum_{s=1}^4 \int_0^3 d\zeta\, \rho_0(\zeta)\varepsilon^{(s)}(\zeta) f(\varepsilon^{(s)}(\zeta)). \quad (29)$$

As a result, the expression for the renormalized bias V takes the following form:

$$V = V_0 + 2\alpha \frac{\partial E(V)}{\partial V}. \quad (30)$$

This equation, together with Eqs. (25) and (26), define the AFM and exciton order parameters as functions of the applied voltage.

B. Analytical results

In this subsection we obtain the solution of Eqs. (25), (26), and (30) in the limits $\Delta_{\mathrm{exc}} \ll \Delta_{\mathrm{AFM}} \ll t_0$ and $T = 0$. When these conditions hold, the functions $\varepsilon^{(1,2)}(\zeta)$ and $\theta(\zeta)$ become

$$\varepsilon^{(1)}(\zeta) \cong -\sqrt{\Delta_{\mathrm{AFM}}^2 + t^2(\zeta - \zeta_0)^2},$$
$$\varepsilon^{(2)}(\zeta) \cong -t(\zeta + \zeta_0), \quad (31)$$
$$\theta(\zeta) \cong \frac{2\Delta_{\mathrm{exc}}t_0 - \Delta_{\mathrm{AFM}}V}{2t^2\zeta_0\zeta},$$

where

$$\zeta_0 = \frac{\sqrt{t_0^2 + V^2/4}}{t}. \quad (32)$$

Substituting $\varepsilon^{(1,2)}(\zeta)$ with $\Delta_{\mathrm{AFM}} = 0$ in Eq. (29), we obtain the following relation between V and V_0:

$$V = \frac{V_0 t}{t + C\alpha\zeta_0}, \quad C = \left.\frac{\partial \rho_0(\zeta)}{\partial \zeta}\right|_{\zeta \to 0} \simeq 0.37. \quad (33)$$

For realistic parameter values, the renormalized bias voltage V depends almost linearly on V_0. Taking $\alpha = 10$ eV, we obtain from Eq. (33) that $V = 0.83V_0$, if $V_0 \ll t_0$. The numerical analysis shows that the estimation $V \approx V_0$ becomes even better for larger values of Δ_{AFM}/t and Δ_{exc}/t.

The analytical expressions for the order parameters are derived in the Appendix. The results can be rewritten as

$$\Delta_{\mathrm{AFM}} = 2t\sqrt{\zeta_0(3-\zeta_0)} \exp\left(-\frac{\frac{4t}{U_0} - \eta_1(\zeta_0) - \frac{\eta_2(\zeta_0)V^2}{4t^2\zeta_0^2}}{2\rho_0(\zeta_0)\frac{t_0^2}{t^2\zeta_0^2}} \right),$$
$$(34)$$

$$\Delta_{\mathrm{exc}} = \Delta_{\mathrm{AFM}}\frac{V}{2t_0} \frac{\frac{4t}{U_0} - \eta_1(\zeta_0) - \eta_2(\zeta_0)\zeta_0}{\frac{4t}{U_{12}} - \frac{4t}{U_0}\frac{t^2\zeta_0^2}{t_0^2} + \frac{V^2(\eta_1(\zeta_0)+\eta_2(\zeta_0)\zeta_0)}{4t_0^2}},$$

where $\eta_1(\zeta_0)$ and $\eta_2(\zeta_0)$ are defined in the Appendix by Eqs. (A5). We see that Δ_{exc} is proportional to the Δ_{AFM}. When $V_0 \ll t_0$, the exciton order parameter depends linearly on V_0.

C. Gap suppression by the transverse bias

The total gap in the spectrum is given by Eq. (22). It coincides with the AFM order parameter if the bias voltage is zero. The dependence of the gap on the ratio U_0/t for zero bias is shown in Fig. 2. The analytical expression Eq. (34) works well for $U_0 \lesssim 2.3t$.

If $V_0 \neq 0$, the exciton order parameter becomes nonzero. The full gap Δ, however, decreases when V_0 increases. The dependence of the full gap Δ on V_0 calculated for three
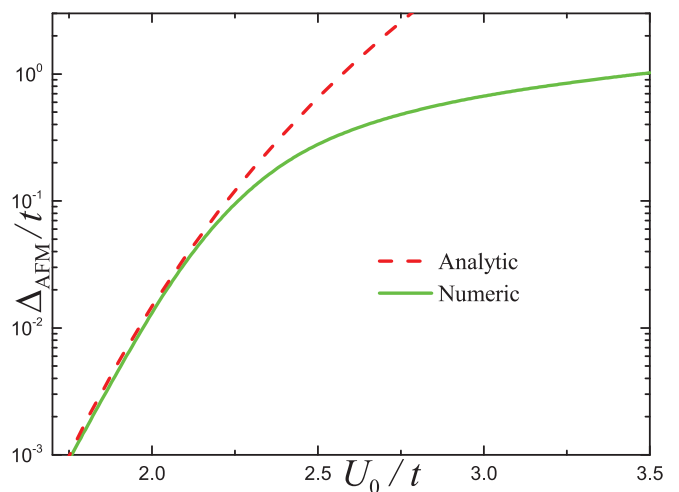

FIG. 2. (Color online) AFM order parameter Δ_{AFM} vs the on-site interaction U_0, for zero bias $V_0 = 0$.
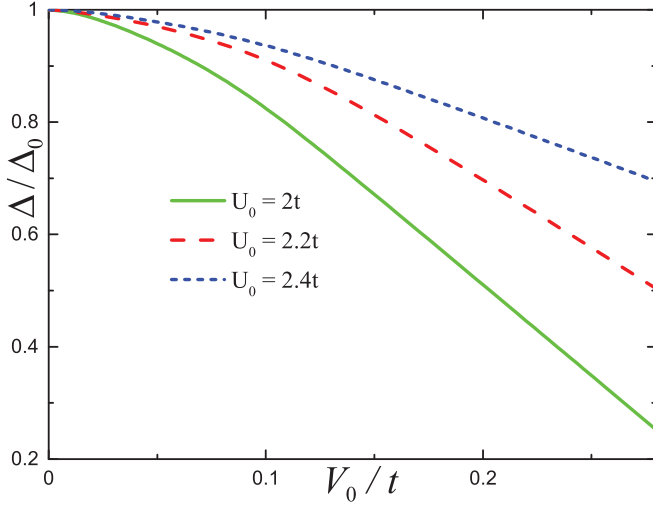
FIG. 3. (Color online) Full gap Δ vs the applied bias V_0, for different values of the on-site Coulomb repulsion U_0. The value Δ_0 is equal to the full gap if $V_0 = 0$, that is, it is the AFM gap Δ_{AFM} for zero bias.

different values of U_0 is shown in Fig. 3. As it follows from this figure, the gap suppression is stronger for smaller U_0.

We consider here only the case of zero temperature. In this case the full gap never reaches zero for realistic values of the applied voltage. At finite temperatures, however, it can be fully suppressed by the bias voltage. This makes it possible to observe a voltage-driven metal-insulator transition.

Let us analyze now the dependencies of the AFM and exciton order parameters on the applied voltage. For the typical values of the system parameters $U_0 \simeq 2.2t$, $U_{12}/U_0 \simeq 1/4$, and $V_0/t_0 \simeq 1$, the values of the order parameters are $\Delta_{\text{AFM}} \simeq 0.17$ eV and $\Delta_{\text{exc}} \simeq 8$ meV. We can rewrite the expressions for the order parameters in terms of magnetizations:

$$S_z = \frac{2\Delta_{\text{AFM}}}{U_0} = \langle n_{n1\mathcal{A}\uparrow} \rangle - \langle n_{n1\mathcal{A}\downarrow} \rangle,$$

$$\phi = \frac{2\Delta_{\text{exc}}}{U_{12}} = \langle d^{\dagger}_{n1\mathcal{A}\uparrow} d_{n2\mathcal{A}\uparrow} \rangle - \langle d^{\dagger}_{n1\mathcal{A}\downarrow} d_{n2\mathcal{A}\downarrow} \rangle. \tag{35}$$

In these equations, the AFM magnetization S_z is equal to the magnetization per site of the sublattice $\mathcal{A}$ in layer 1. For the G-type AFM order, the magnetizations of electrons located at neighboring sites have opposite signs.

The exciton magnetization ϕ can be viewed as the spin located on the link connecting the sites $A1$ and $A2$ (for definitions of $A1$ and $A2$, see Fig. 1). The spin on the link connecting carbon atoms $B1$ and $B2$ has the opposite sign. The dependence of S_z on the applied bias voltage calculated for three different values of the on-site interaction constant U_0 is shown in Fig. 4 by the solid lines. This magnetization is suppressed by the bias voltage. The suppression is stronger for smaller U_0. When $U_0 > 2.4t$, the magnetization S_z only slightly depends on V_0. The exciton magnetization ϕ is shown in Fig. 4 by dashed lines. It increases almost linearly with V_0. Nevertheless, ϕ is much smaller than S_z, even for relatively large V_0.
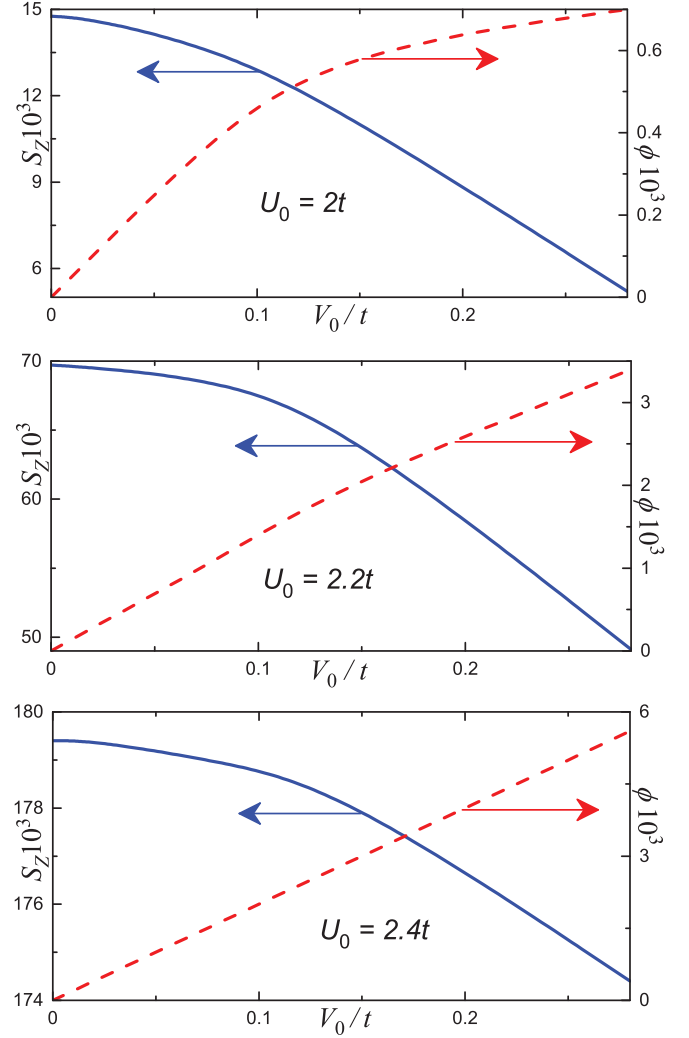

FIG. 4. (Color online) The dependence of the AFM magnetization S_z and of the exciton magnetization ϕ on the bias voltage V_0 for three different values of the on-site interaction U_0. The blue continuous curves are the AFM magnetization S_z, while the red dashed curves are for the exciton magnetization ϕ. For all panels we use the value $U_{12} = U_0/4$.

D. Exciton order parameter

In the limit of small interactions $U_{12} \ll U_0 \ll t$, the second equation in Eq. (34) simplifies and reduces to

$$\Delta_{\text{exc}} = \Delta_{\text{AFM}} \frac{V}{2t_0} \frac{U_{12}}{U_0}. \tag{36}$$

In this limit the value of the exciton order parameter depends linearly on the interplane repulsion U_{12}. References [25–29,36] considered a system with two graphene layers separated by an insulating layer. The dielectric barrier between the layers completely suppresses the interlayer tunneling and destroys the AFM order. In this case, the value of the exciton order parameter depends exponentially on the Coulomb interaction between the layers. Under such conditions, according to Ref. [36], the exciton gap becomes exponentially small around 1 mK. In this case, a small amount of disorder makes exciton condensation impossible [37]. In our case, the exciton order parameter depends almost linearly on U_{12}. Thus, the exciton

order parameter can exist in our system even if the interplane interaction is rather small.

Can we detect this order parameter? In principle, the exciton condensation can be observed experimentally by measuring the Coulomb drag [24,38,39]. The experimental observation of Coulomb drag in bilayer graphene systems with a dielectric barrier between the layers has been reported [40]. The execution and interpretation of a similar experiment on bilayer graphene without the insulating layer might be a much more complicated issue. Also, angle-resolved photoemission spectroscopy and scanning tunneling microscopy can be used to probe the exciton phase in such bilayer system [41].

All the above results were obtained at zero temperature. The detailed study of the temperature dependence of the AFM order parameter at zero-bias voltage was performed in Ref. [22]. Since the graphene bilayer is a two-dimensional system, it does not have a distinct magnetic phase transition. However, we can define a crossover temperature T^* between the short-range antiferromagnetic and paramagnetic states. The calculations done in Ref. [22] show that $T^* \approx 0.5\Delta_{\mathrm{AFM}}$. For realistic values of the applied voltage the exciton order parameter is much smaller than the AFM order parameter. Consequently, $\Delta_{\mathrm{exc}} \ll T^*$. However the exciton order parameter is tied with the AFM order parameter, and we expect that they both have the same crossover temperature T^*. Since the AFM order parameter can be high enough, the exciton order parameter can survive at relatively high temperatures.

E. Effect of doping

The contact of the sample with the substrate and/or electrodes can induce a finite carrier density in the conduction or valence band. This effect could be enhanced by the bias voltage. The doping violates the perfect nesting of the electron and hole Fermi surfaces. In Refs. [21,22] it was shown that doping reduces the AFM order parameter:

$$\Delta_{\mathrm{AFM}}(x) = \Delta_{\mathrm{AFM}}\sqrt{1 - \frac{x}{x_c}},$$
$$x_c = \frac{\Delta_{\mathrm{AFM}}\rho_0(\zeta_0)}{2t}, \tag{37}$$

where $x = n - 1$ is the doping level and n is the number of the electrons per site. Generalization of Eq. (37) for the finite bias is obvious for the case $V \ll t_0$: we should use the functions $\zeta_0(V)$ and $\Delta_{\mathrm{AFM}}(V)$ given by Eqs. (32) and (34). We can expect that the physics does not changes significantly in the case $V \sim t_0$. Since $\Delta_{\mathrm{exc}} \propto \Delta_{\mathrm{AFM}}$, the dependence of the exciton order parameter on x has the form $\Delta_{\mathrm{exc}}(x) = \Delta_{\mathrm{exc}}\sqrt{1 - x/x_c}$. The main effect of the doping is the suppression of the AFM and exciton order parameters. The large doping, $x > x_c$, destroys the order parameters, turning the system into a metallic phase.

In general, the value of doping x depends on the bias voltage V. However, the explicit formula for $x(V)$ depends on the material and design of the substrate and electrodes and could not be derived in a general case.

As it was shown in Ref. [22], the electronic liquid of the AA-BLG becomes inhomogeneous in certain ranges of doping and temperatures. Such a phase-separated state is a mixture of undoped AFM insulator and metal. Study of this phase in a transverse electric field is an interesting question that lies beyond the scope of this article.

IV. CONCLUSIONS

In this paper we have studied theoretically the electronic properties of biased AA-stacked bilayer graphene. The model Hamiltonian was analyzed in the mean-field approximation. At zero bias, the ground state of the system is antiferromagnetic. We found that the applied transverse voltage stabilizes the exciton order parameter coexisting with the AFM order. This new order parameter couples the electrons and holes in different graphene layers. The AFM phase with the coexisting exciton order parameter is the most stable phase if the bias voltage is nonzero. The electronic gap is partially suppressed by the bias voltage, leading to a tunable metal-insulator transition. The value of the exciton order parameter can be about several tens of meV. Despite this small value, the exciton order parameter can survive at relatively high temperatures due to its coexistence with the AFM phase. However, a sufficiently large value of the doping can induce an inhomogeneous electronic state and even destroy order parameters.

APPENDIX: ANALYTIC SOLUTION

Here we derive the analytical formulas for the AFM and exciton order parameters. We introduce dimensionless quantities $\delta_{\mathrm{AFM}} = \Delta_{\mathrm{AFM}}/t$ and $\delta_{\mathrm{exc}} = \Delta_{\mathrm{exc}}/t$. It is convenient to rewrite the exciton order parameter in the following form:

$$\delta_{\mathrm{exc}} = \delta_{\mathrm{AFM}}\frac{V}{2t_0}b, \tag{A1}$$

where b is the new variable. Using this substitution we can rewrite Eqs. (25) and (26) in the form

$$\frac{4t}{U_0} = \int_0^3 d\zeta\, \rho_0(\zeta)\left[\frac{1}{\sqrt{\delta_{\mathrm{AFM}}^2 + (\zeta - \zeta_0)^2}} + \frac{1}{\zeta + \zeta_0}\right] - \int_0^3 d\zeta\, \rho_0(\zeta)\frac{V^2(1-b)}{4t^2\zeta_0\zeta}\left[\frac{1}{\sqrt{\delta_{\mathrm{AFM}}^2 + (\zeta - \zeta_0)^2}} - \frac{1}{\zeta + \zeta_0}\right], \tag{A2}$$

$$\frac{4t}{U_{12}} = \int_0^3 d\zeta\, \rho_0(\zeta)\left[\frac{1}{\sqrt{\delta_{\mathrm{AFM}}^2 + (\zeta - \zeta_0)^2}} + \frac{1}{\zeta + \zeta_0}\right] + \int_0^3 d\zeta\, \rho_0(\zeta)\frac{t_0^2(1-b)}{t^2\zeta_0\zeta b}\left[\frac{1}{\sqrt{\delta_{\mathrm{AFM}}^2 + (\zeta - \zeta_0)^2}} - \frac{1}{\zeta + \zeta_0}\right]. \tag{A3}$$

Taking the integration in Eq. (A2) we obtain in the limit $\delta_{\text{AFM}} \ll 1$

$$\frac{4t}{U_0} = \rho_0(\zeta_0)\left(1 - \frac{V^2(1-b)}{4t^2\zeta_0^2}\right)\ln\left(\frac{4\zeta_0(3-\zeta_0)}{\delta_{\text{AFM}}^2}\right) + \eta_1(\zeta_0) + \frac{V^2(1-b)}{4t^2\zeta_0}\eta_2(\zeta_0) + O\left(\delta_{\text{AFM}}^2\right), \quad \text{(A4)}$$

where

$$\eta_1(\zeta_0) = \int_0^3 d\zeta \left[\frac{\rho_0(\zeta)}{\zeta + \zeta_0} + \frac{\rho_0(\zeta) - \rho_0(\zeta_0)}{|\zeta - \zeta_0|}\right],$$

$$\eta_2(\zeta_0) = \int_0^3 \frac{d\zeta}{\zeta}\left[\frac{\rho_0(\zeta)}{\zeta + \zeta_0} - \frac{\rho_0(\zeta)\zeta_0 - \rho_0(\zeta_0)\zeta}{\zeta_0\,|\zeta - \zeta_0|}\right]. \quad \text{(A5)}$$

Performing a similar integration in Eq. (A3) and expressing the logarithmic term using Eq. (A4) we obtain in the limit of small $b \ll 1$ the following equation for b:

$$b = \frac{\frac{4t}{U_0} - \eta_1(\zeta_0) - \eta_2(\zeta_0)\zeta_0}{\frac{4t}{U_{12}} - \frac{4t}{U_0}\frac{t^2\zeta_0^2}{t_0^2} + \frac{V^2(\eta_1(\zeta_0) + \eta_2(\zeta_0)\zeta_0)}{4t_0^2}}. \quad \text{(A6)}$$

For the range of parameters U_0 and U_{12} under study, we have $b < 0.05$, so the assumption $b \ll 1$ is well satisfied. The expression for Δ_{exc} is written as follows:

$$\Delta_{\text{exc}} = \Delta_{\text{AFM}}\frac{V}{2t_0}\frac{\frac{4t}{U_0} - \eta_1(\zeta_0) - \eta_2(\zeta_0)\zeta_0}{\frac{4t}{U_{12}} - \frac{4t}{U_0}\frac{t^2\zeta_0^2}{t_0^2} + \frac{V^2(\eta_1(\zeta_0) + \eta_2(\zeta_0)\zeta_0)}{4t_0^2}}. \quad \text{(A7)}$$

The antiferromagnetic gap is found from Eq. (A4), where we can neglect b in the first and third terms. As a result, we obtain

$$\Delta_{\text{AFM}} = 2t\sqrt{\zeta_0(3-\zeta_0)}\exp\left(\frac{\eta_1(\zeta_0) + \frac{\eta_2(\zeta_0)V^2}{4t^2\zeta_0^2} - \frac{4t}{U_0}}{2\rho_0(\zeta_0)\frac{t_0^2}{t^2\zeta_0^2}}\right). \quad \text{(A8)}$$

[1] A. H. Castro Neto, F. Guinea, N. M. R. Peres, K. S. Novoselov, and A. K. Geim, Rev. Mod. Phys. **81**, 109 (2009).

[2] D. S. L. Abergel, V. Apalkov, J. Berashevich, K. Ziegler, and T. Chakraborty, Adv. Phys. **59**, 261 (2010).

[3] A. V. Rozhkov, G. Giavaras, Y. P. Bliokh, V. Freilikher, and F. Nori, Phys. Rep. **503**, 77 (2011).

[4] E. McCann and V. I. Fal'ko, Phys. Rev. Lett. **96**, 086805 (2006); E. V. Castro, N. M. R. Peres, T. Stauber, and N. A. P. Silva, *ibid.* **100**, 186803 (2008); R. Nandkishore and L. Levitov, *ibid.* **104**, 156803 (2010); Phys. Rev. B **82**, 115124 (2010); F. Zhang, H. Min, M. Polini, and A. H. MacDonald, *ibid.* **81**, 041402(R) (2010).

[5] Y. Lemonik, I. L. Aleiner, C. Toke, and V. I. Fal'ko, Phys. Rev. B **82**, 201408(R) (2010); O. Vafek and K. Yang, *ibid.* **81**, 041401(R) (2010); J. Nilsson, A. H. Castro Neto, N. M. R. Peres, and F. Guinea, *ibid.* **73**, 214418 (2006).

[6] S. Novoselov, E. McCann, S. V. Morozov, V. I. Fal'ko, M. I. Katsnelson, U. Zeitler, D. Jiang, F. Schedin, and A. K. Geim, Nat. Phys. **2**, 177 (2006); S. Latil and L. Henrard, Phys. Rev. Lett. **97**, 036803 (2006); B. Partoens and F. M. Peeters, Phys. Rev. B **74**, 075404 (2006); H. Min, B. Sahu, S. K. Banerjee, and A. H. MacDonald, *ibid.* **75**, 155115 (2007).

[7] B. E. Feldman, J. Martin, and A. Yacoby, Nat. Phys. **5**, 889 (2009).

[8] A. S. Mayorov, D. C. Elias, M. Mucha-Kruczynski, R. V. Gorbachev, T. Tudorovskiy, A. Zhukov, S. V. Morozov, M. I. Katsnelson, V. I. Fal'ko, A. K. Geim, and K. S. Novoselov, Science **333**, 860 (2011).

[9] E. V. Castro, K. S. Novoselov, S. V. Morozov, N. M. R. Peres, J. M. B. Lopes dos Santos, J. Nilsson, F. Guinea, A. K. Geim, and A. H. Castro Neto, Phys. Rev. Lett. **99**, 216802 (2007).

[10] Y. Zhang, T.-T. Tang, C. Girit, Z. Hao, M. C. Martin, A. Zettl, M. F. Crommie, Y. R. Shen, and F. Wang, Nature (London) **459**, 820 (2009).

[11] H. Fukidome, M. Kotsugi, K. Nagashio, R. Sato, T. Ohkochi, T. Itoh, A. Toriumi, M. Suemitsu, and T. Kinoshita, Sci. Rep. **4**, 3713 (2014).

[12] C.-H. Park and S. G. Louie, Nano Lett. **10**, 426 (2010).

[13] P. L. de Andres, R. Ramírez, and J. A. Vergés, Phys. Rev. B **77**, 045403 (2008).

[14] E. Prada, P. San-Jose, L. Brey, and H. Fertig, Solid State Commun. **151**, 1075 (2011).

[15] C. W. Chiu, S. H. Lee, S. C. Chen, F. L. Shyu, and M. F. Lin, New J. Phys. **12**, 083060 (2010).

[16] Y.-H. Ho, J.-Y. Wu, R.-B. Chen, Y.-H. Chiu, and M.-F. Lin, Appl. Phys. Lett. **97**, 101905 (2010).

[17] Z. Liu, K. Suenaga, P. J. F. Harris, and S. Iijima, Phys. Rev. Lett. **102**, 015501 (2009).

[18] J. Borysiuk, J. Soltys, and J. Piechota, J. Appl. Phys. **109**, 093523 (2011).

[19] J.-K. Lee, S.-Ch. Lee, J.-P. Ahn, S.-Ch. Kim, J. I. B. Wilson, and P. John, J. Chem. Phys. **129**, 234709 (2008).

[20] A. L. Rakhmanov, A. V. Rozhkov, A. O. Sboychakov, and F. Nori, Phys. Rev. Lett. **109**, 206801 (2012).

[21] A. O. Sboychakov, A. L. Rakhmanov, A. V. Rozhkov, and F. Nori, Phys. Rev. B **87**, 121401(R) (2013).

[22] A. O. Sboychakov, A. V. Rozhkov, A. L. Rakhmanov, and F. Nori, Phys. Rev. B **88**, 045409 (2013).

[23] J. P. Eisenstein and A. H. MacDonald, Nature (London) **432**, 691 (2004).

[24] D. Nandi, A. D. K. Finck, J. P. Eisenstein, L. N. Pfeiffer, and K. W. West, Nature (London) **488**, 481 (2012).

[25] C.-H. Zhang and Y. N. Joglekar, Phys. Rev. B **77**, 233405 (2008).

[26] H. Min, R. Bistritzer, J.-J. Su, and A. H. MacDonald, Phys. Rev. B **78**, 121401 (2008).

[27] A. Perali, D. Neilson, and A. R. Hamilton, Phys. Rev. Lett. **110**, 146803 (2013).

[28] J. Zhang and E. Rossi, Phys. Rev. Lett. **111**, 086804 (2013).

[29] Y. E. Lozovik, S. L. Ogarkov, and A. A. Sokolik, Phys. Rev. B **86**, 045429 (2012).

[30] S. Banerjee, L. Register, E. Tutuc, D. Reddy, and A. Mac-Donald, IEEE Electron Device Lett. **30**, 158 (2009).

[31] J.-C. Charlier, J.-P. Michenaud, and X. Gonze, Phys. Rev. B **46**, 4531 (1992).

[32] H. J. Xiang, E. J. Kan, S.-H. Wei, X. G. Gong, and M.-H. Whangbo, Phys. Rev. B **82**, 165425 (2010); B. S. Pujari, S. Gusarov, M. Brett, and A. Kovalenko, *ibid.* **84**, 041402(R) (2011); L. Openov and A. Podlivaev, Semiconductors **46**, 199 (2012); Physica E **44**, 1894 (2012); Tech. Phys. **57**, 1603 (2012).

[33] T. O. Wehling, E. Şaşıoğlu, C. Friedrich, A. I. Lichtenstein, M. I. Katsnelson, and S. Blügel, Phys. Rev. Lett. **106**, 236805 (2011); A. Du, Y. H. Ng, N. J. Bell, Z. Zhu, R. Amal, and S. C. Smith, J. Phys. Chem. Lett. **2**, 894 (2011).

[34] M. Schuler, M. Rosner, T. O. Wehling, A. I. Lichtenstein, and M. I. Katsnelson, Phys. Rev. Lett. **111**, 036601 (2013).

[35] R. P. Feynman, Phys. Rev. **56**, 340 (1939).

[36] M. Yu. Kharitonov and K. B. Efetov, Semicond. Sci. Technol. **25**, 034004 (2010).

[37] D. S. L. Abergel, M. Rodriguez-Vega, E. Rossi, and S. Das Sarma, Phys. Rev. B **88**, 235402 (2013).

[38] E. H. Hwang, R. Sensarma, and S. Das Sarma, Phys. Rev. B **84**, 245441 (2011).

[39] J. Su and A. H. MacDonald, Nature Physics **4**, 799 (2008).

[40] R. V. Gorbachev, A. K. Geim, M. I. Katsnelson, K. S. Novoselov, T. Tudorovskiy, I. V. Grigorieva, A. H. MacDonald, S. V. Morozov, K. Watanabe, T. Taniguchi, and L. A. Ponomarenko, Nature Physics **8**, 896 (2012).

[41] S. Rist, A. A. Varlamov, A. H. MacDonald, R. Fazio, and M. Polini, Phys. Rev. B **87**, 075418 (2013).